

Study of CNN deep learning model for temporal remote sensing data processing to map rabi crops

Mragank Snighal^{1,*}, Ashish Payal² and Anil Kumar³

^{1,2} USIC&T, Guru Gobind Singh Indraprastha University, New Delhi, India

³ Indian Institute of Remote Sensing, Dehradun, India

*Email: mraganksinghal@gmail.com

(Received: Dec 5, 2021; In final form: 25 Sep 2022)

Abstract: Convolution Neural Network (CNN) is a deep learning approach that has become an area of interest to the researchers for solving complex problems. With the evaluation of CNN, extraction of deep features for accurate classification of remotely sensed images has gained lot of momentum. This research work uses CNN deep learning model for mapping rabi crops (mustard and wheat) using temporal remote sensing data. The mappings of mustard and wheat crops have been conducted using multispectral temporal images obtained from Sentinel 2A/2B between the dates 1st Nov 2019 and 24th Feb 2020 of Banasthali, Rajasthan region. The CNN model created in this research work uses several layers along with 5 activation functions (relu, sigmoid, tanh, elu and selu) for finding out which activation function gave the best result for the proposed study. Batch size has been examined from 1 to 50 in the multiple of 5 and epochs have been tested from 1 to 10 for a training data of 200 samples for each class. The optimal value with a batch size of 5 and epochs of 30 has been calculated as best suited in this study as the accuracy was getting constant. The implementation of CNN model for classification shows better results as compared to the traditional approach as the CNN algorithms are learning algorithms. This also helps in handling the heterogeneity within a class. A comparison has been conducted using Modified Possibilistic *c*-Means (MPCM) fuzzy algorithm for the classification of the same set of classes. F-Score, Kappa and Overall Accuracy have been calculated to show how the proposed approach has been outperformed and the level of classification accuracy achieved.

Keywords: Convolution Neural Network (CNN), Deep feature extraction, multispectral image classification, Soft Classification

1. Introduction

Digital image classification is one of the prominent application domains to map and extract the data of remote areas through satellite imagery. Lillesand and Kiefer (2015) have mentioned digital image classification as a quantitative technique to classify image data into various categories. Supervised and unsupervised image classifications are two broad categories of classification procedure (Campbell, 1996). When training data is available, supervised classification is widely used and when training data is unavailable, unsupervised classification is applied on remote sensing imagery. Higher accuracy can be achieved with the intervention of computers to process a digital image (Richards and Jia, 2013).

Bezdek et al. (1984) presented Fuzzy *c*-Means (FCM) algorithm with a thought of fuzzy sets to solve mixed pixel problem. Later, to overcome the drawbacks of FCM, Krishnapuram et al. (1993) proposed an algorithm based on a possibilistic concept and improvement in the objective function, which was labeled as Possibilistic *c*-means (PCM). Fuzzy based classifiers are generally effective in handling mixed pixels to produce precise and reasonable outcomes from image classification (Chawla, 2010).

Supervised noise clustering (NC) has been opted as the base classifier. Adding nine different kernel functions as the distance functions resulting in a kernel-based classifier, termed KNC (Sengupta et al. 2019). Li et al. (2003) revised the objective function of PCM, and an efficient clustering algorithm, named Modified Possibilistic *c*-Means

(MPCM), was presented by him. This algorithm saves an amount of running time by eliminating the computation of membership parameters in every iteration. Since PCM causes a coincident cluster problem, MPCM was introduced to fit the clusters, closer to one another. As compared to PCM, MPCM is less sensitive to noise and avoids trivial solutions too (Li et al., 2003).

PCM and MPCM algorithms are capable of mapping specific classes of interest from temporal datasets (Misra et al., 2012; Singh et al., 2019). The reflectance from these classes depends upon several factors such as soil type, terrain, moisture content, and atmospheric condition (Rawat et al., 2021). A single date image may have spectral overlap between two or more classes while mapping the second/third classification level. This spectral overlap can effectively be separated by the use of temporal images (Chandola et al., 2010).

Traditional classifiers are not capable to map single class of interest from remote sensing image. ID-CNN model implemented in this research work has been designed to map only wheat or mustard from given temporal remote sensing data. So, this specific single class mapping capabilities of ID-CNN model has been explored in this research work, which is not there with traditional image classifiers. Secondly, the accuracy and reliability of the information gathered by the imagery is dependent on the classification. Although there are some advanced classification methods such as Support Vector Machines, Random Forest, etc., which have been used widely traditionally, but still the researchers have been still working to improve the classification accuracy because the classified images provide important base information for

GIS applications and analysis on decision making process. The gap in the traditional approach was the loss of information and also lack of learning algorithms that were addressed with the help of learning algorithms like CNN (Mustafa et al., 2016).

Many fields of science, remote sensing included, were able to exploit the success of natural image classification by Convolutional Neural Network (CNN) models using a technique commonly called transfer learning (Lima et al., 2019). Hu et al. (2015) remarked that the performance of remote- sensing image classification has only slightly improved in recent years. The main reason remote- sensing image classification only marginally improved is due to the fact that the approaches relying on low- level features are incapable of generating sufficiently powerful feature representations for remote- sensing scenes (Lima et al., 2019). Hu et al. (2015) concluded that the more representative and higher- level features, which are abstractions of the lower- level features, are desirable and play a dominant role in the scene classification task.

Convolutional Neural Networks (CNNs) mostly improve prediction performance using big data and plentiful computing resources and have pushed the boundaries of what was possible. Problems which were assumed to be unsolvable are now being solved with super-human accuracy (Mahony et al., 2019). Current progress in deep-learning models, specifically deep convolutional neural networks (CNN) architectures, have improved the state-of- the- art in visual object recognition and detection, speech recognition and many other fields of study (Cun et al. 2015). Many CNN models use 10 to hundreds of layers. Huang et al. (2016) proposed models with thousands of layers (Huang et al., 2016). Due to the vast number of operations performed in deep CNN models, it is often difficult to discuss the interpretability, or the degree to which a decision taken by a model can be interpreted.

Remote Sensing images have features at many layers which can be extracted using deep feature extraction methods. Many classifiers are designed for classification but at a single layer, there some classifiers which also work on two layers such as decision tree or kernel SVMs (Bengio et al., 2013). Despite CNNs' powerful feature extraction capabilities, Hu et al. (2015) and others found that in practice it is difficult to train CNNs with small datasets. However, Yosinski et al. (2014) and Yin et al. (2017) observed that the parameters learned by the layers in many CNN models trained on images exhibit a very common behavior.

This research work experimented classification with a CNN model which has been applied on temporal remote sensing data to map rabi crops and compared using Modified Possibilistic *c*-Means (MPCM) algorithm. The proposed CNN approach has been compared with Euclidean and variance-covariance parameters in the MPCM classifier. Secondly, spectral overlaps between classes like mustard and wheat have been handled using the temporal indices database. This temporal indices database for each class has been generated during the class-based sensor independent (CBSI)-NDVI approach

and compared with NDVI temporal database. Convolutional Neural Networks (CNNs) do not generate statistical parameters from training samples. In place of generating statistical training parameters, CNN considers all training samples as it is, so that each sample can give equal impact on training the model as well as classify unknown pixel in an image. Due to this, outputs from CNN models are very homogeneous. Due to this factor 1D-CNN model has been tested in this research work.

2. Vegetation indices

Many scientists have extracted and modelled various vegetation biophysical variables using remote sensing data since 1960. Various efforts have been taken towards developing vegetation indices, which are defined as dimensionless, radiometric measures that function as indicators of relative abundance and activity of green vegetation. Although there are more than 20 different vegetation indices in use, in this research work, NDVI has been considered. Cohen (1991) suggests that the first true vegetation index was the *Simple Ratio (SR)*, which is the near – infrared (*NIR*) to red reflectance ratio described in Birth and Mc-Vey (1968) as mentioned in Eq. (2.1):

$$SR = \frac{NIR}{Red} \quad (2.1)$$

Rouse et al. (1974) developed the generic *Normalized Difference Vegetation Index (NDVI)* as mentioned in Eq. (2.2):

$$NDVI = \frac{NIR - Red}{NIR + Red} \quad (2.2)$$

Temporal indices datasets can provide spectral change over time for a crop (Upadhyay et al., 2012). Band ratio is used in remote sensing to eliminate the different topography and illumination effects and enhance a class (Sengar et al., 2001). The *NDVI* was widely used and applied to the original Landsat MSS digital remote sensing data. A novel Class-Based Sensor-Independent Indices (*CBSI*) generates a much-enhanced class of interest in indices data (Upadhyay et al., 2013). The advantage of using CSBI approach in indices generation is that, user does not have to provide bands in given indices formula. CBSI have minimum and maximum operators which selects bands such a way that class of interest get maximum enhancement. It has also been used to reduce the spectral dimensionality of temporal remote sensing dataset which has been used in this study as well. The *CBSI-NDVI* formula is mentioned in Eq. (2.3):

$$CBSI - NDVI = \frac{\rho_{max} - \rho_{min}}{\rho_{max} + \rho_{min}} \quad (2.3)$$

where ρ_{max} and ρ_{min} represent the band of maximum and minimum reflectance, respectively.

3. Mathematical concept of classification algorithm

MPCM has been introduced to resolve the limitations of FCM and PCM. MPCM has fast clustering ability, abilities to resist noise, and trivial solution (Li et al, 2003). Since PCM causes coincident clusters, thus MPCM is proposed to overcome this problem and fit the clusters, which are

close to one another. Li et al. (2003) introduced the main limitation of PCM that it takes more time in implementation, and a large number of parameters need to be determined. This section will present the mathematical concepts of the MPCM algorithm and its objective function formulation. Li et al. (2003) revised the objective function of PCM, presented an efficient clustering algorithm, and discussed how to choose parameters.

Pseudo code of MPCM Algorithm

1. Assign mean values of each class from training data.
2. Assign the value of the degree of fuzziness $\infty > m > 1$.
3. Compute the regularization parameter ‘ η_i ’ as mentioned in Eq. (3.6).
4. Compute the membership matrix, as given in Eq. (3.1):

$$u_{ij} = e^{\left(\frac{-d_{ij}^2}{\eta_i}\right)}, \text{ where } d_{ij}^2 = \|x_i - v_j\| \quad (3.1)$$

5. Assign the final class to each pixel.

To minimize the impact of noise and outlier’s parameter λ_i was introduced for each training sample, and the modification has been done in PCM's objective function. The objective function of MPCM is mentioned in Eq. (3.2):

$$J_m = \sum_{i=1}^N \sum_{j=1}^C (\mu_{ji})^m \|x_i - v_j\|^2 + \sum_{i=1}^N \eta_i \sum_{j=1}^C (\lambda_i - \mu_{ji})^m \quad (3.2)$$

λ_i is taken according to the expression mentioned in (3.3):

$$\lambda_j = \sum_{i=1}^C \exp\{-\alpha \|x_j - \beta_i\|^2\} \quad \lambda_i > 0 \quad (3.3)$$

where α is a suitably chosen constant, and

$$\beta_i = \sum_{j=1}^N w_{ij} x_j / \sum_{j=1}^N w_{ij}, \text{ where } w_{ij} \text{ is a monotonous decreasing function.}$$

4. CNN model

Convolutional neural network is a class of deep learning methods which has become dominant in various computer vision tasks and is attracting interest across a variety of domains, including image classification. CNN is designed to automatically and adaptively learn spatial hierarchies of features through backpropagation by using multiple building blocks, such as convolution layers, pooling layers, and fully connected layers (Yamashita et al., 2018).

A CNN is composed of a stacking of several building blocks: convolution layers, pooling layers (e.g., max pooling), and fully connected (FC) layers. A model’s performance under particular kernels and weights is calculated with a loss function through forward propagation on a training dataset, and learnable parameters, i.e., kernels and weights, are updated according to the loss value through backpropagation with gradient descent optimization algorithm, ReLU, rectified

linear unit. An overview of a convolutional neural network (CNN) architecture and the training process is shown in Figure 1.

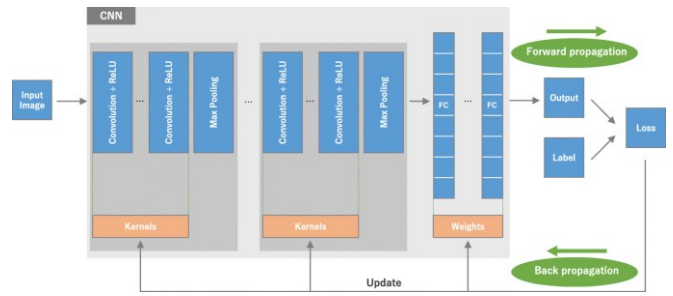


Figure 1. CNN Architecture

The CNN architecture includes several building blocks, such as convolution layers, pooling layers, and fully connected layers. A typical architecture consists of repetitions of a stack of several convolution layers and a pooling layer, followed by one or more fully connected layers. In this research work, two 1D convolution layers are used which reduces the in-plane dimensionality of the feature maps in order to introduce a translation invariance to small shifts and distortions, and decrease the number of subsequent learnable parameters. The max pooling layer extracts patches from the input feature maps, outputs the maximum value in each patch, and discards all the other values. Once the features extracted by the convolution layers and down-sampled by the pooling layers are created, they are mapped by a subset of fully connected layers to the final outputs of the network, such as the probabilities for each class in classification tasks. The final fully connected layer has the same number of output nodes as the number of classes. Each fully connected layer is followed by a nonlinear function, ReLU (Rectified Linear Activation Unit). The CNN Model used in this research work is shown in Figure 2.

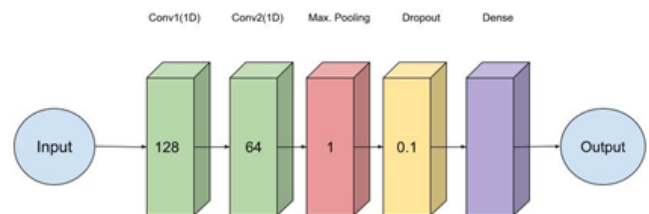


Figure 2. CNN Model used

MPCM algorithm has fast clustering abilities and also it can resist noise and trivial solutions. With each layer, the CNN’s complexity in understanding the image increases. This means that layers at the beginning are responsible for detecting low-level features such as edges and colors and the layers at the end are responsible for detecting high-level features such as shapes that we can easily recognize. The main advantage of CNNs compared to a traditional neural network is that they automatically detect important features without any human supervision.

5. Study area and dataset used

This section elaborates the details about the study area and the dataset used in this research work.

5.1. Study area

Surroundings of the Banasthali Vidyapith area, Rajasthan state, India, have been selected as the study area for this research to identify mustard and wheat fields while testing the proposed approach. Banasthali is located in the district Tonk and is surrounded by agricultural land where mustard covers around 2,99,000 hectares of area, whereas wheat is cultivated in approximately 66,000 hectares. Several other crops such as barley, gram, jowar, bajra, moong and urd can also be found in comparatively less area. The area is located in the north-eastern part in the state of Rajasthan. The study area lies between 26°23' and 26°24' north latitude, 75°51' and 75°54' east longitude. It is surrounded by Jaipur towards the north, Sawai Madhopur towards the east, Kota district on the southeast, Bundi towards the south, Bhilwara district on the southwest, and Ajmer towards the west.

The reasons for selecting this study area were:

- The area is surrounded by small villages where mustard, wheat, and grass fields can be found easily.
- During November (2019) and December (2019) large fields of mustard can be seen here, which later becomes fallow land by the end of March (2020).

The different classes of interest i.e., mustard and wheat ground truth samples were collected from the field visit which has been shown in Figure 3. The location map and different land cover classes identified in the study area are presented in Figure 4.

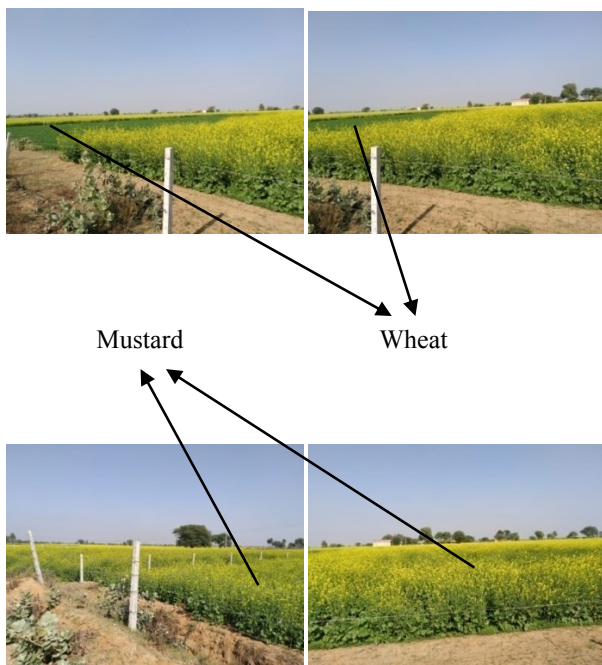


Figure 3. Photographs taken during the field visit on 11th Dec 2019 in the surroundings of Banasthali Vidyapith region

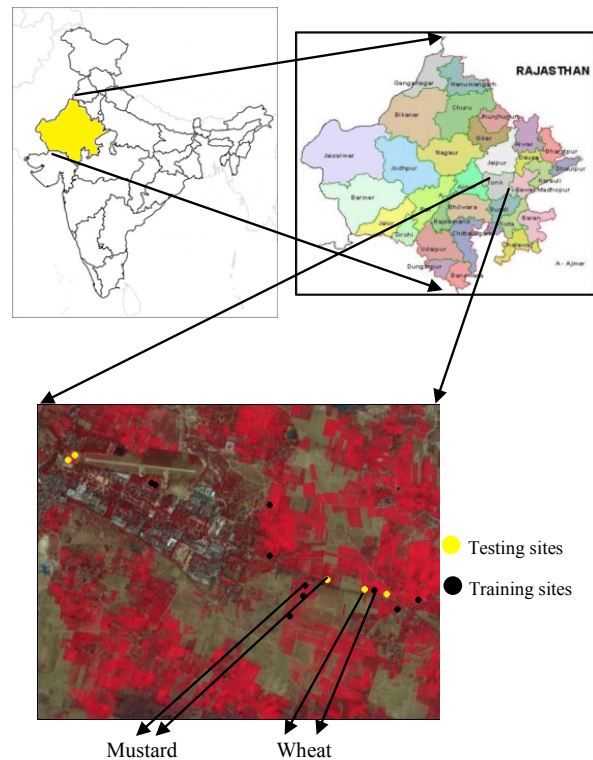


Figure 4. Location of study, Banasthali Vidyapith area, Rajasthan State, India

Table 1 shows the latitude and longitude locations of various field samples collected during the field visit done on 11th Dec 2019 in the Banasthali Vidyapith region's surroundings. Around the field, 200 samples were identified at different locations for these classes of interest. Ten fields of mustard and wheat classes and a total of twenty field samples have been shown in Table 1, from where training pixels were collected. Table 2 shows ten field samples that have been used for reference data.

Table 1. Ground Truth Samples Collected during the field visit

Classes->	Mustard		Wheat	
Samples	Latitude	Longitude	Latitude	Longitude
Sample 1	26°23'49"	75°53'08"	26°23'45"	75°53'36"
Sample 2	26°23'47"	75°53'21"	26°23'45"	75°53'36"
Sample 3	26°23'43"	75°53'34"	26°23'47"	75°53'38"
Sample 4	26°23'44"	75°53'35"	26°23'47"	75°53'38"
Sample 5	26°23'44"	75°53'40"	26°25'51"	75°52'30"
Sample 6	26°23'41"	75°53'45"	26°25'46"	75°52'31"
Sample 7	26°23'43"	75°53'40"	26°25'45"	75°52'32"
Sample 8	26°23'40"	75°53'46"	26°25'21"	75°52'37"
Sample 9	26°23'59"	75°53'13"	26°25'18"	75°52'38"
Sample 10	26°23'44"	75°53'31"	26°25'15"	75°52'38"

Table 2. Reference Data Collected during the field visit

Classes->	Mustard		Wheat	
Samples	Latitude	Longitude	Latitude	Longitude
Sample 1	26°25'06"	75°52'08"	26°25'21"	75°52'23"
Sample 2	26°25'03"	75°51'45"	26°25'24"	75°52'36"
Sample 3	26°25'04"	75°51'43"	26°25'02"	75°52'38"
Sample 4	26°25'02"	75°52'38"	26°25'01"	75°52'48"
Sample 5	26°24'58"	75°52'25"	26°24'55"	75°52'51"

5.2. Dataset used

In this research work, the multispectral temporal images from twin satellites i.e., Sentinel-2A and Sentinel-2B have been used to discriminate mustard and wheat fields. Seven temporal images have been acquired from 1st Nov 2019 to 24th Feb 2020 of the same area. These images were then used to study the CNN deep learning model’s performance. The multispectral temporal Sentinel 2A/2B dataset and its sensor specification have been given in Table 3.

Table 3. Sentinel 2A/2B dataset and sensor specification.

Specifications	Sentinel – 2A/B
Spatial Resolution	10 – 60 meters
Spectral Resolution	13 bands
Scene Size	290 km x 290 km
Image Acquired on	1-Nov-19, 16-Nov-19, 11-Dec-19, 26-Dec-19, 10-Jan-20, 30-Jan-20, 24-Feb-20

6. Methodology

Initially, multispectral images have been pre-processed to generate temporal indices database using Sentinel–2A/B satellite images. CBSI-NDVI approach has been applied to generate a temporal indices database parallel to it. The objective of generating temporal indices database was to reduce the spectral dimension of temporal images and maintain temporal dimension to incorporate phonological profile of crop, and represented in the form of vector elements to be used in MPCM classifier. Spectral dimension was reduced, and only the temporal dimension used in a fuzzy-based classifier to have input data representing indices as vector elements. Temporal indices database has been used in separability analysis, using Euclidean separability, to find out the best temporal date combination for separating mustard and wheat fields, as shown in table (4) and (5). Once suitable dates for each class were identified, using these dates, temporal indices database was generated.

The temporal indices database was used as an input to the CNN Model to generate the classified outputs for mustard and wheat fields. The temporal indices database was also used in the supervised Modified Possibilistic *c*-Means (MPCM) algorithm for accuracy assessment. A detailed description of the methodology has been given in Figure 5.

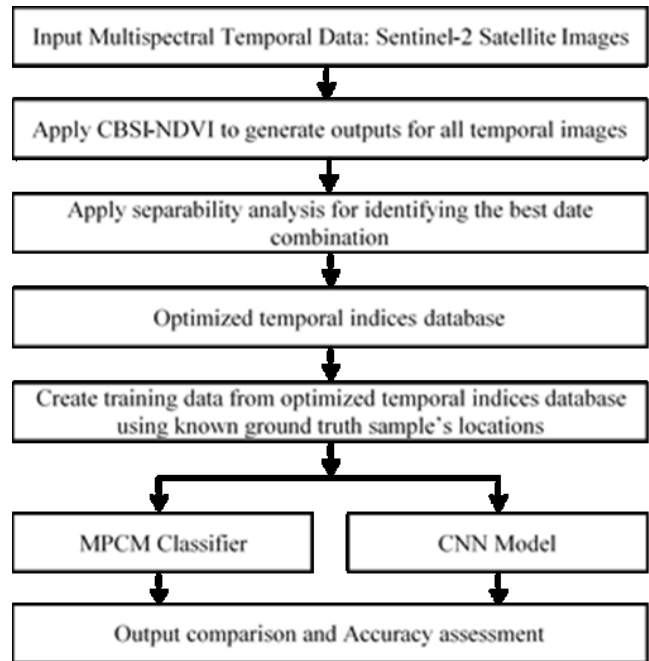


Figure 5. Methodology Adopted

Following steps were applied to identify mustard and wheat fields’ classes using temporal dataset of 1st Nov 2019, 16th Nov 2019, 11th Dec 2019, 26th Dec 2019, 10th Jan 2020, 30th Jan 2020, and 24th Feb 2020 images:

- 1) All temporal images were used to generate CBSI-NDVI outputs using seed training data for mustard and wheat fields separately, with the help of the CBSI-NDVI formula mentioned in Eq. (2.3).
- 2) Outputs from step (1) were used in separability analysis to identify temporal images suitable to be used for any specific class.
- 3) Temporal images identified in step (2) were then used to generate CBSI-NDVI outputs using seed training data for mustard, wheat, and grass fields separately in a similar way as done in step (1).
- 4) The outputs generated in step (3) were used to create an optimized temporal indices database.
- 5) Training data was created from the optimized temporal indices database generated from step (4) using the ground truth samples locations.
- 6) The optimized temporal indices database (generated from step 4) was then classified using training data created in step (5), by applying CNN Model and MPCM classifier.
- 7) The classified outputs from step (6) were then compared, and an accuracy assessment was conducted.
- 8) The same steps were applied to generate classified outputs for other classes of interest.

As discussed in the methodology, Table 4 and Table 5 gives information about bands and optimized temporal dates used for mustard, wheat, and grass classes as identified from step (2).

Table 4. Selected Bands for Mustard using CBSI-NDVI approach

Dates	Mustard		
	CBSI-NDVI value	ρ_{max}	ρ_{min}
1-Nov-19	0.57	SWIR	Blue
16-Nov-19	0.4	VNIR	Blue
11-Dec-19	0.62	VNIR	SWIR
30-Jan-20	0.86	VNIR	Blue
24-Feb-20	0.52	VNIR	SWIR

Table 5. Selected Bands for Wheat using CBSI-NDVI approach

Dates	Wheat		
	CBSI-NDVI value	ρ_{max}	ρ_{min}
11-Dec-19	0.52	VNIR	Blue
26-Dec-19	0.81	VNIR	Blue
10-Jan-20	0.89	VNIR	Red
30-Jan-20	0.91	VNIR	Blue
24-Feb-20	0.72	VNIR	SWIR

The graph in Figure 6 represents the CBSI-NDVI values of mustard for the suitable temporal dates using CBSI-NDVI as shown in Table 4. Similarly, the graph in Figure 7 represents the CBSI-NDVI values of wheat for the suitable temporal dates using CBSI-NDVI as shown in Table 5. Since the suitable dates of mustard are different from wheat, therefore, CBSI-NDVI values have been shown in two graphs.

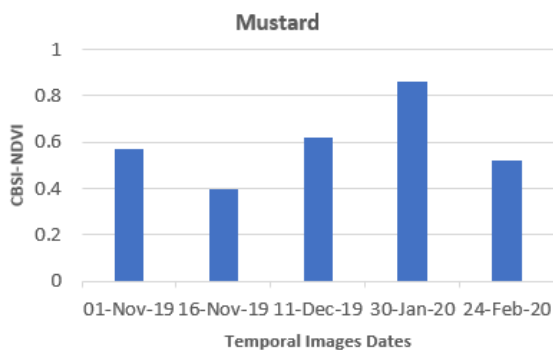


Figure 6. Graphical representations of CBSI-NDVI values for mustard

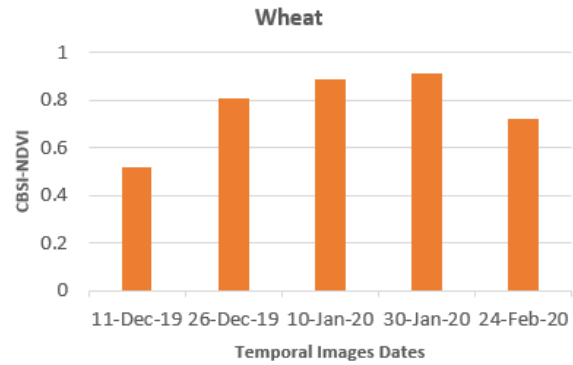


Figure 7. Graphical representations of CBSI-NDVI values for wheat

7. Results and discussion

To identify the mustard and wheat fields in the Banasthali area of Rajasthan state, temporal remote sensing data for seven different dates have been available. The seed training samples of temporal datasets were collected, which were applied on 1st Nov 2019, 16th Nov 2019, 11th Dec 2019, 26th Dec 2019, 10th Jan 2020, 30th Jan 2020 and 24th Feb 2020 temporal images. Separability analysis has been conducted for mustard, wheat, and grass fields to identify suitable optimum temporal images for classification.

For model generalization training data was used to train the model, validation ground samples were used to validate the 1D-CNN model. Testing samples as unknown pixels were used to classify the temporal indices data. Classified output was assessed through collecting testing samples from classified outputs while comparing it with training sample outputs, to find out generalization performance of 1D-CNN model.

Figure 8 shows the mustard fields' output by using MPCM classifier and CNN Model using the selected temporal images. Figure 9 shows the wheat fields' output by using MPCM classifier and CNN Model using the selected temporal images.

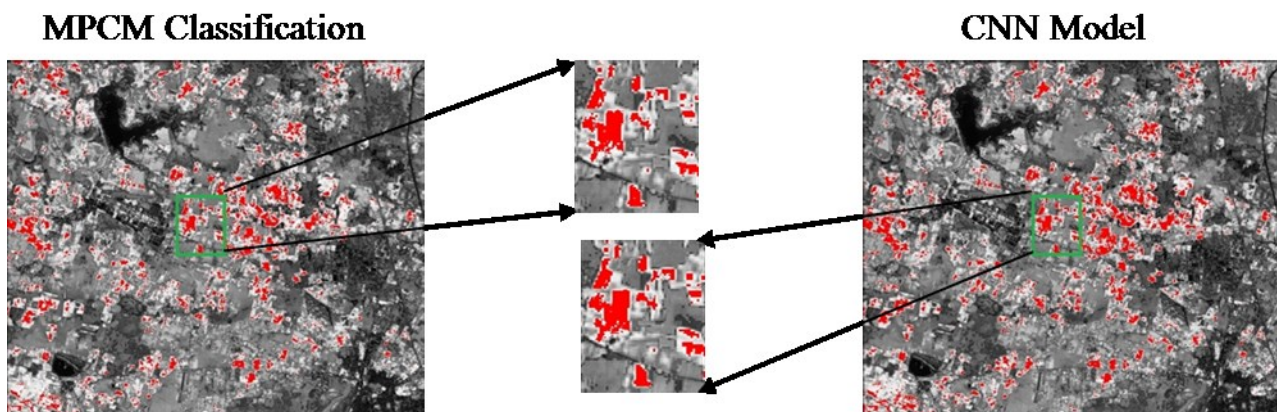


Figure 8. Mustard class output using MPCM and CNN model

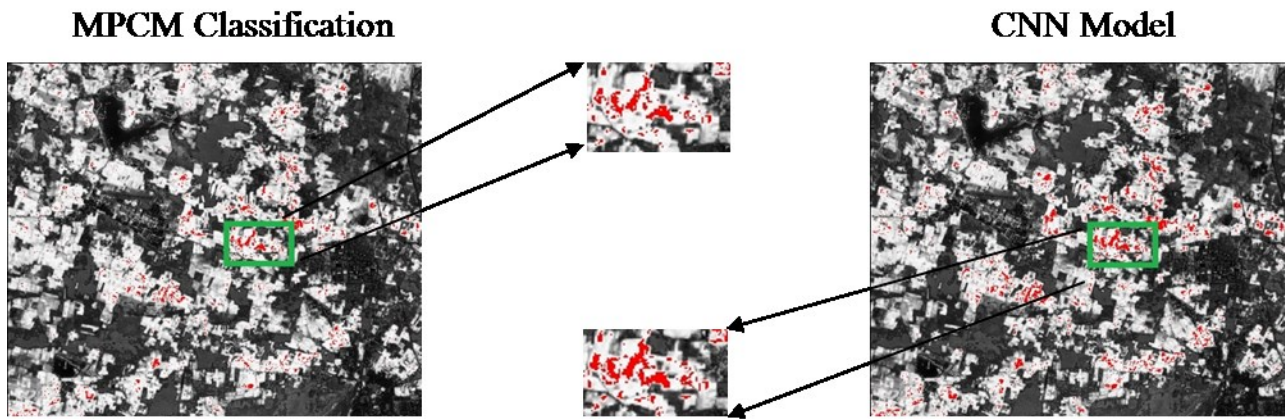


Figure 9. Wheat class output using MPCM and CNN model

Figure 10 shows the optimized CNN model for performance. Batch size has been examined from 1 to 50 in the multiple of 5 and epochs have been tested from 1 to 10 for a training data of 200 samples for each class. The optimal value with a batch size of 5 and epochs of 30 has been calculated as best suited in this study as the accuracy was getting constant.

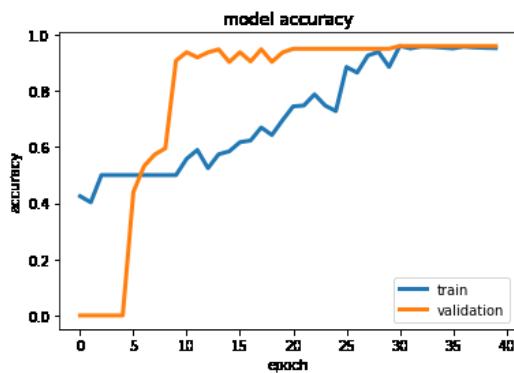


Figure 10. Optimized CNN performance model

Table 6 shows the mean-membership difference (MMD) between favorable and non-favorable classes using different methodologies for quantitative comparison between traditional and proposed approaches. MMD is an independent approach for the stability of the concerned class by calculating the mean difference of membership value of the concerned class and other classes of pure pixel (Singh et al., 2021).

Table 6. Mean-Membership Difference (MMD) between favorable and non-favorable classes

MMD using MPCM Classifier			
Favourable Classes		Non-Favourable Classes	
Mustard-Mustard	0.03	Mustard-Wheat	0.27
Wheat-Wheat	0.02	Wheat-Mustard	0.22
MMD using CNN Model			
Favourable Classes		Non-Favourable Classes	
Mustard-Mustard	0.01	Mustard-Wheat	0.42
Wheat-Wheat	0.01	Wheat-Mustard	0.74

Using the quantitative comparison from table 6, with the help of mean-membership difference, it can be concluded that the CNN model was capable of yielding better results as compared with MPCM classifier. Table 7 shows the accuracy assessment using F-Score, Kappa, and Overall Accuracy using different methodologies for qualitative comparison between traditional and proposed approaches.

Table 7. Accuracy Assessment through F-Score and Overall accuracy

Using MPCM Classification					
Class	Precision	Recall	F-Score	Kappa	Overall Accuracy
Mustard	0.92	0.90	0.91	0.80	90.0
Wheat	0.91	0.84	0.88	0.74	87.0
Using CNN Model					
Mustard	0.93	0.96	0.94	0.88	94.0
Wheat	0.92	0.92	0.92	0.84	92.0

Overall accuracy which is mentioned in Table 7 also supports the same conclusion of the proposed approach compared to the traditional MPCM classification.

8. Conclusions

This study has integrated CNN deep learning model for temporal remote sensing data processing. The proposed approach uses CNN model for the processing of mustard and wheat crops using temporal datasets. Identification of these classes has been carried out using temporal datasets obtained from Sentinel 2A/2B between the dates 1st Nov 2019 and 24th Feb 2020.

The classification results of optimized temporal indices database with MPCM and CNN model were studied. The CNN model outperformed the traditional MPCM approach. From this research it can be concluded that CNN model gave the best classification results for the mapping of mustard and wheat fields.

References

Bengio Y, A. Courville and P. Vincent (2013). Representation learning. A review and new perspectives. IEEE Trans. Pattern Anal. Mach. Intell, 35(8), pp 1798–1828.

- Bezdek J. C., R. Ehrlich and W. Full (1984). FCM: The fuzzy c-means clustering algorithm. *Computers & Geosciences*, 10 (2), 191–203. Available: doi:10.1016/0098-3004(84)90020-7
- Birth G. S. and G. R. McVey (1968). Measuring the Color of Growing Turf with a Reflectance Spectrophotometer. *American Society of Agronomy*, 60, 640-643. Available: <https://doi.org/10.2134/agronj1968.00021962006000060016x>
- Campbell J. B. (1996). *Introduction to Remote Sensing*, 2nd ed. Guilford Press, pp 337–349.
- Chandola V. and R. Vatsavai (2010). Multi-temporal remote sensing image classification - A multi-view approach. *Proceedings of the 2010 Conference on Intelligent Data Understanding, CIDU*, pp 258-270.
- Chawla S. (2010). Possibilistic c-means-spatial contextual information based sub-pixel classification approach for multi-spectral data. University of Twente Faculty of Geo-Information and Earth Observation (ITC), Enschede.
- Cohen W. B (1991). Temporal versus spatial variation in leaf reflectance under changing water stress conditions. *International Journal of Remote Sensing*, 12(9), 1865–1876. Available: doi:10.1080/01431169108955215
- Cun L., Y. Bengio G. Hinton (2015). Deep learning. *Nature*. 521, 436–444. Available: doi:10.1038/nature14539
- Hu F., G. Xia, J. Hu and L. Zhang (2015). Transferring Deep Convolutional Neural Networks for the Scene Classification of High-Resolution Remote Sensing Imagery. *Remote Sens.* 7, 14680–14707. Available: doi:10.3390/rs71114680
- Huang G., Y. Sun, Z. Liu, D. Sedra and K. Weinberger (2016). Deep Networks with Stochastic Depth. *Proceedings of the 14th European Conference, Amsterdam, The Netherlands*.
- Krishnapuram R. and J. M. Keller (1993). A possibilistic approach to clustering. *IEEE Transactions on Fuzzy Systems*, 1(2), 98–110. Available: doi:10.1109/91.227387.
- Li K., H. Huang and K. Li (2003). A modified PCM clustering algorithm. *International conference on machine learning and cybernetics*, 2, 1174-1179. Available: doi:10.1109/ICMLC.2003.1259663
- Lillesand T. M. and R. W. Kiefer (2015). *Remote Sensing and Image Interpretation*, 7th ed. Wiley & Sons, NJ, pp 485–608.
- Lima P., Rafael and Marfurt (2019). Convolutional Neural Network for Remote-Sensing Scene Classification: Transfer Learning Analysis. *Remote Sensing*, 12, 86. Available: doi:10.3390/rs12010086
- Mahony N. O., S. Campbell and A. Carvalho (2019). Deep Learning vs. Traditional Computer Vision. *Advances in Computer Vision Proceedings of the 2019 Computer Vision Conference (CVC)*. Springer Nature Switzerland AG, pp. 128-144. Available: doi: <https://doi.org/10.1007/978-3-030-17795-9>
- Misra G., A. Kumar, R. Patel, R., Zurita and A. Singh (2012). Mapping specific crop-A multi sensor temporal approach. *International Geoscience and Remote Sensing Symposium (IGARSS), IEEE International*, 3034-3037. Available: doi:10.1109/IGARSS.2012.6350786
- Mustafa U., M. Esetlili, S. Balik, Fusun, S. Abdikan and Y. Kurucu (2016). Comparison of crop classification methods for the sustainable agriculture management. *Journal of environmental protection and ecology*, 17, 648–655.
- Rawat A., A. Kumar and P. Upadhyay (2021). A Comparative Study of 1D-Convolutional Neural Networks with Modified Possibilistic c-Mean Algorithm for Mapping Transplanted Paddy Fields Using Temporal Data. *J Indian Soc Remote Sens.* Available: doi: 10.1007/s12524-020-01303-4
- Richards J. A. and X. Jia (2013). *Remote Sensing Digital Image Analysis*, 4th ed. Springer-Verlag Berlin Heidelberg, pp 295-332.
- Rouse J. W., R. H. Haas, J. A. Schell and D.W. Deering (1974). Monitoring vegetation systems in the Great Plains with ERTS. *Third Earth Resources Technology Satellite-1 Symposium*, 1, NASA SP-351, NASA, Washington, D.C., 309-317.
- Sengar S. S., A. Kumar, S. K. Ghosh, H. R. Wason and P. S. Roy (2001). Liquefaction identification using class-based sensor independent approach based on single pixel classification after 2001 Bhuj, India earthquake. *Journal of Applied Remote Sensing*, 6(1):063531-1-063531-13. Available: doi:10.1117/1.JRS.6.063531
- Sengupta I., A. Kumar and R. Dwivedi (2019). Performance Evaluation of Kernel-Based Supervised Noise Clustering Approach. *Journal of the Indian Society of Remote Sensing*, 47. Available: doi:10.1007/s12524-019-00938-2.
- Singh A. and A. Kumar (2019). Fuzzy Based Approach to Incorporate Spatial Constraints in Possibilistic c-Means Algorithm for Remotely Sensed Imagery. *International Conference on Sustainable Computing in Science, Technology & Management, Jaipur*. Available: <http://dx.doi.org/10.2139/ssrn.3354465>
- Singh A., A. Kumar and P. Upadhyay (2021). A novel approach to incorporate local information in Possibilistic c-Means algorithm for an optical remote sensing imagery, *The Egyptian Journal of Remote Sensing and Space Science*, 24 (1), pp 151-161, ISSN 1110-9823. Available: doi: 10.1016/j.ejrs.2020.06.001
- Upadhyay P., A. Kumar, P. S. Roy, S. K. Ghosh and I. Gilbert (2012). Effect on specific crop mapping using WorldView-2 multispectral add-on bands: soft classification approach. *Journal of Applied Remote Sensing*, 6(1):063524-1-063524-15. Available: doi:10.1117/1.jrs.6.063524
- Upadhyay P., S. K. Ghosh and A. Kumar (2013). High resolution temporal normalized difference vegetation indices for specific crop identification. *ISPRS - International Archives of the Photogrammetry, Remote Sensing and Spatial Information Sciences*, XL-1/W1, 351-

355. Available: 10.5194/isprsarchives-XL-1-W1-351-2013

Yamashita R., M. Nishio and R. K. G. Do (2018). Convolutional neural networks: an overview and application in radiology. *Insights Imaging* 9, 611–629. Available: <https://doi.org/10.1007/s13244-018-0639-9>

Yin X., W. Chen, X. Wu and H. Yue (2017). Fine-tuning and visualization of convolutional neural networks.

Proceedings of the 2017 12th IEEE Conference on Industrial Electronics and Applications (ICIEA), Siem Reap, Cambodia, pp. 1310–1315. Available: doi:10.1109/ICIEA.2017.8283041

Yosinski, J., J. Clune, Y. Bengio and H. Lipson (2014). How transferable are features in deep neural networks? Proceedings of the 27th International Conference on Neural Information Processing Systems, Montreal, QC, Canada, Volume 27, pp. 3320–3328.